International Gas Union Research Conference 2011

A new experimentally tested method to classify gaseous fuels for knock resistance based on the chemical and physical properties of the gas

Authors

S. Gersen, M.H. Rotink, G.H.J. van Dijk
KEMA
P.O. Box 2029
9704 CA Groningen
The Netherlands

H.B. Levinsky
KEMA and
University of Groningen
The Netherlands

Abstract

In this paper we present a new method to classify the knock resistance of natural gas mixed with different fractions of ethane, propane and hydrogen and compare the predictions with experiments on a modern medium-BMEP CHP-unit gas engine. The knock propensity of the gases, which is directly related to the autoignition behavior of the fuels have been studied based on numerically calculated autoignition delay times of the gaseous fuels.

Analyses of the measurements in the gas engine show that variations in the fuel composition cause differences in the in-cylinder pressure and temperature history, which affect the autoignition behavior, and can result in quantitatively different knock behavior with varying gas composition. Towards this end the entire temperature history of the end-gas is taken into account into the autoignition calculations. The pressure and temperature history can be modeled based on the observation that the measured combustion phasing correlates very well with the numerical calculated laminar burning velocity for both the studied natural gas/H_2 and the natural gas/C_2H_6/C_3H_8 mixtures. Interestingly, the correlation between the combustion phasing and the burning velocity for the natural gases/H_2 mixtures scales with a different correlation factor than the natural gas mixed with fractions of added ethane and propane. Knock predictions and measurements by using the knock limited spark timing (*KLST*) show the reduction in knock resistance with increasing fractions of hydrogen, ethane and propane in the fuel. Comparison between the knock propensity based on the calculated autoignition delay time and the measured knock propensity (*KLST*) show excellent agreement for all measured fuels. The knock propensity calculated by the AVL-List methane number shows good agreement with the knock measurements for the higher hydrocarbon containing natural gas mixtures but shows large disagreement with the knock propensity measurements for natural gas/hydrogen mixtures.

Future work is planned for validating the method for other fuels and larger engine types.

TABLE OF CONTENTS

1 INTRODUCTION

One of the consequences of the growing production of unconventional gases, the globalization of the energy market and the drive towards sustainability is that gases with significantly different composition can be or will be traded and distributed. For example, “rich” natural gases that contain substantial larger concentrations of higher hydrocarbons than the traditional pipeline gas are being introduced into grids, as are “sustainable” gases, such as biogas, which can contain large fractions of hydrogen, CO and CO_2. When these gases are used to fuel reciprocating internal combustion engines these variations in gas composition can induce the occurrence of engine knock. The latter phenomenon is characterized by spontaneous ignition (autoignition) of unburned fuel mixture, the so-called end-gas, ahead of the propagating flame in the engine cylinder. Engine knock should be avoided since it can physically damage the engine and increase pollutant emissions [1]. Because optimal operating conditions (low emissions, high efficiency and maximum power output) is often close to those of knock occurrence it is of great importance to know the knock resistance of a fuel accurately.

In the last decades several empirical methods, such as the AVL-list methane number, have been developed to classify fuels with respect to their knock sensitivity [2]. In the methane number (MN) the knock propensity of fuels is compared with an equivalent methane/hydrogen mixture; methane, which has the highest knock resistance, has a MN of 100, at the opposite end of the scale, hydrogen, which has the lowest knock resistance, has the lowest MN of 0. The first draw back of this method is that the methane number is derived from knock measurements performed on a stoichiometrically operating engine, while the actual diversity of installed engines is great, and modern engines tend to operate substantially fuel lean at different pressure and temperature conditions of the compressed end gas. As shown in [3-8] the autoignition behavior of fuels seem to depend strongly on the specific regime of temperature and pressure in a given engine. This observation serves as a caveat that using a single ranking system, as is the current use of the Methane Number, may be a too-simple representation of the actual situation. Furthermore, it is not clear how well the existing, empirical, methods to characterize knock correctly account for exotic fuel components, such as hydrogen or CO. A fundamentally sound method to assess the knock tendency of fuels can remove much uncertainty regarding the limits of validity of the current methods.

In this paper we present a new method to classify the knock resistance of gaseous fuels and compare the predictions with experiments on the modern medium-BMEP-CHP-unit gas engine. The method is based on the knowledge that knock is directly related to autoignition of the end-gas before being consumed by the flame and it takes into account the changes in in-cylinder conditions (P,T) experienced by the end gas as results of the varying gas composition.

On the one hand, the method is valuable for the (international) gas industry, allowing the assessment of gas interchangeability without compromising the safe and efficient operation of gas engines in mobile and stationary applications. On the other hand, the method should provide a valuable tool for the gas engine manufacturers to define knock-free gas engine performance ratings for today's and tomorrow's fuel gases.

2 EXPERIMENTAL PROCEDURE

A 210 kW 1500 rpm lean-burn turbo-charged intercooled 6-cylinder gas engine for CHP-duties was used in this study. The motor management system and further instrumentation allowed for precise adjustment, monitoring and acquisition of power output, fuel consumption, exhaust gas emissions, ignition timing, air-fuel-ratio and other relevant engine parameters.

The in-cylinder pressures were measured with a Kistler type 6052 piezoelectric pressure sensors and a Kistler type 5011 charge amplifiers connected to a Smetec Combi-Pro indication system. A crankshaft-mounted pulse generator provided 0.1 ^{o}CA resolution for the cylinder pressure data acquisition. The Combi-Pro system was also used for knock detection through monitoring of the maximum amplitude of pressure oscillations in the HP-filtered cylinder pressure data in a window of consecutive cycles. Thresholds settings used were 2 bar for the amplitude and 30 cycles for the window. The knock limit was arbitrarily chosen at one only (cluster of) knock event(s) within a 15 minute steady-state test run.

During the experiments, fuel for the test engine was delivered by a mobile gas mixing unit. This unit allows on-stream variation of the fuel gas composition by independent adjustment of the mass flow rates of up to six source gas streams. The fuel compositions used in the experiments are Dutch natural gas mixtures mixed with ethane, propane (table 1) and hydrogen (table 2). All mixture compositions were verified by gas chromatography. Once the composition fuel/air mixtures at a lambda, λ of 1.5 (φ=0.67) and the other relevant cylinder parameters are set (table 1 and 2) the pressure traces of the gases at non-knocking condition are measured at a constant spark timing of 14° before top dead center (BTDC). Subsequently, the spark timing was gradually varied up to the point of the onset of borderline knock; this point is called Knock Limited Spark Timing (KLST). Figure 1 shows the test engine and the mobile gas mixing unit.

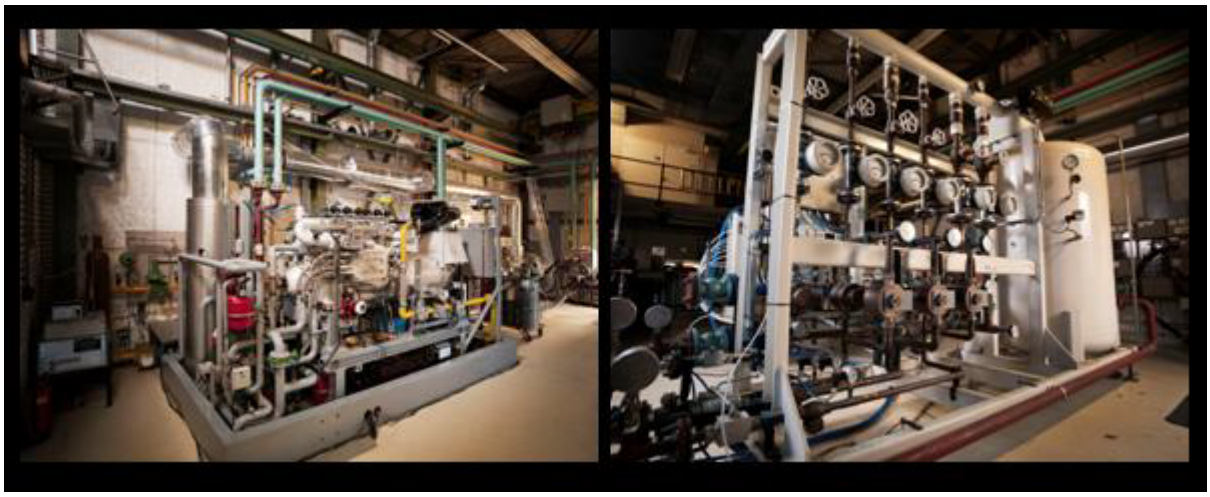

Figure 1. The 210 kW test engine (left) and the mobile gas mixing unit (right) in KEMA's Combustion Laboratory.

Table 1: Composition of rich natural gases studied

	A	B	C	D	E	F	G
CH_4	81.827	80.744	79.828	75.211	67.209	74.462	65.350
C_2H_6	2.664	4.413	2.699	11.048	20.425	2.502	12.281
C3H8	0.369	0.395	3.106	0.369	0.325	9.128	10.187
n-C4H10	0.058	0.062	0.080	0.059	0.067	0.085	0.161
i-C4H10	0.0	0.0	0.074	0.0	0.053	0.142	0.0
n-C5H12	0.017	0.019	0.018	0.018	0.015	0.015	0.014
i-C5H12	0.026	0.108	0.018	0.019	0.016	0.016	0.015
+C6	0.055	0.062	0.062	0.058	0.053	0.054	0.045
H2	0	0	0	0	0	0	0
He	0.048	0.047	0.047	0.044	0.039	0.045	0.037
N2	14.005	13.242	13.187	12.325	11.05	12.700	11.160
CO_2	0.931	0.909	0.880	0.851	0.749	0.852	0.752
LHV	31.663	32.529	33.566	34.627	37.784	37.105	40.984
KLST	24	22.5	20.0	19.5	17.5	16.0	14
Ti, K	366.0	366.4	366.4	366.9	366.3	366.0	366.5
Pi, bar	2.16	2.11	2.15	2.11	2.09	2.11	2.07

Table 2: Composition of hydrogen/natural gas mixtures

	H	I	J	K	L	M
CH4	81.92	79.36	76.87	73.08	68.94	65.46
C2H6	2.93	2.84	2.76	2.64	2.48	2.35
C3H8	0.44	0.43	0.42	0.40	0.38	0.36
n-C4H10	0.08	0.08	0.08	0.07	0.07	0.07
i-C4H10	0.07	0.07	0.06	0.06	0.06	0.06
n-C5H12	0.02	0.02	0.02	0.02	0.02	0.02
i-C5H12	0.02	0.02	0.02	0.03	0.02	0.02
+C6	0.07	0.07	0.07	0.07	0.06	0.06
H2	0	3.14	6.18	10.86	15.94	20.19
He	0.02	0.04	0.04	0.04	0.01	0.00
N2	13.42	12.99	12.56	11.89	11.21	10.64
CO2	0.96	0.94	0.91	0.86	0.82	0.78
LHV	35.50	34.79	34.11	33.07	31.92	30.96
KLST	23	22	21	19.5	18.0	17.0
Ti, K	366.3	366.3	366.0	366.3	366.5	366.7
Pi, bar	2.15	2.16	2.13	2.10	2.09	2.1

3 SIMULATION PROCEDURE OF ENGINE KNOCK

Knock in spark ignited engines occurs when the compressed unburned fraction of fuel/air mixture in the cylinder, the so called end gas, ignites spontaneously before being consumed by the propagating flame front initiated by the spark plug. By calculating autoignition of the end gas which is constantly compressed by both the propagation of the flame front and mechanical compression by the piston we simulated the occurrence of engine knock during the cycle with the program SENKIN [9]. The chemical mechanism [10-14] used in the simulations is validated based on autoignition delay time measurements for methane/ethane/propane/butane/pentane mixtures [13, 14] and optimized for $CH_4/H_2/CO$ mixtures measured in a Rapid Compression Machine (RCM) at temperatures relevant to engines [15].

Based on the specific volume of the end gas the simulation model computes the combined pressure, temperature and chemical history of the end-gas during the compression and combustion phase of a cycle for a given fuel. The specific volume of the end gas is derived from a measured or simulated non-knocking pressure history, by assuming adiabatic compression of the unburned end gas by using the following equations,

$$\int_{T_i(t_0)}^{T(t)} \frac{\gamma}{\gamma - 1} d\ln T = \ln \frac{P(t)}{P_i(t_o)} \tag{1}$$

$$\ln(CR) = \ln\left(\frac{V_i(t_0)}{V(t)}\right) = \int_{T_i(t_0)}^{T(t)} \frac{1}{\gamma - 1} d\ln T \tag{2}$$

where T_i and P_i are the intake temperature and pressure, $P(t)$ is the pressure of the unburned gas mixture, $T(t)$ is the temperature of the unburned gas mixture, V_i is the specific volume of the adiabatic core of the unburned gas at the start of the compression stroke and is taken arbitrary, $V(t)$ is the temporary specific adiabatic core volume of the unburned mixture and $\gamma(T)$ is the ratio of temperature-dependent specific heat capacities of the unburned mixture (C_p/C_v). Clearly, with the measured cylinder pressure traces typically being from non-knocking engine operation, the simulation model will not predict auto-ignition of the end-gas for any of the given fuels and thus not allow ranking them in terms of the above stated delay time. To overcome this, we increased, artificially, the the intake manifold temperature of the mixture until knock occurs in the simulations, assuming that this increase has a negligible effect on the pressure trace. Here we defined knock when autoignition of the unburned end gas occurs before the flame completely consumed the end gas. More specifically, in the simulations we increased the manifold intake temperature with 47K such that in the simulation of the reference fuel auto-ignition occurs near the end of the combustion phase, the latter (somewhat arbitrarily) positioned at the 90% apparent heat release timing. Clearly, simulations for fuels with a lower knock resistance than the reference gas A show auto-ignition earlier in the cycle. The calculated pressure spike depicted in figure 2 indicates the occurrence of knock of reference gas A. In addition figure 2 shows the definition of the auto-ignition delay time.

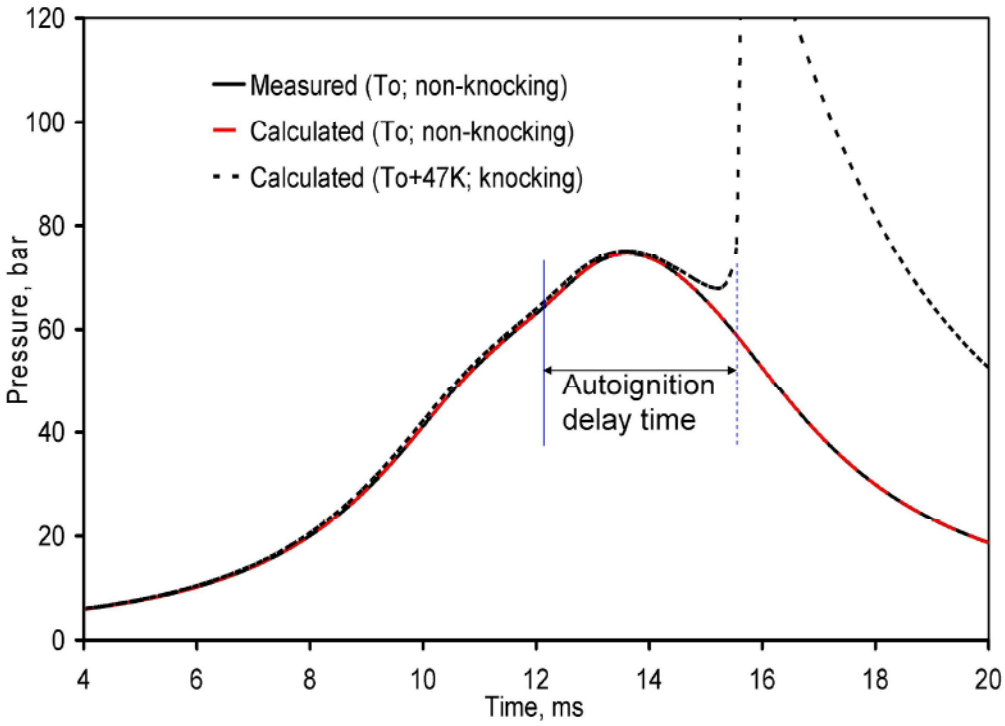

Figure 2. *Measured pressure history and calculated autoignition of gas A subjected to the complete measured pressure and temperature history, at (fictive) initial temperature T_0+47K.*

4 RESULTS AND DISCUSSION

Figure 3 shows the pressure profiles of the Dutch natural gas/H_2 mixtures (table 2) measured under non-knocking conditions. The measurements show that the peak pressure and temperature increase substantially with increasing fraction hydrogen in Dutch natural gas. Since the autoignition behavior of fuels is very sensitive to temperature and moderately sensitive to pressure it is necessary to take into account the changes in the pressure and temperature history of the end gas as a result of varying gas composition into the engine knock simulations. Towards this end, engine knock simulations for the natural gas mixtures mixed with ethane and propane (figure 4) and hydrogen (figure 5) have been performed based on the effective volume derived from the measured cylinder pressures of the gases at non-knocking conditions, as described in the previous section.

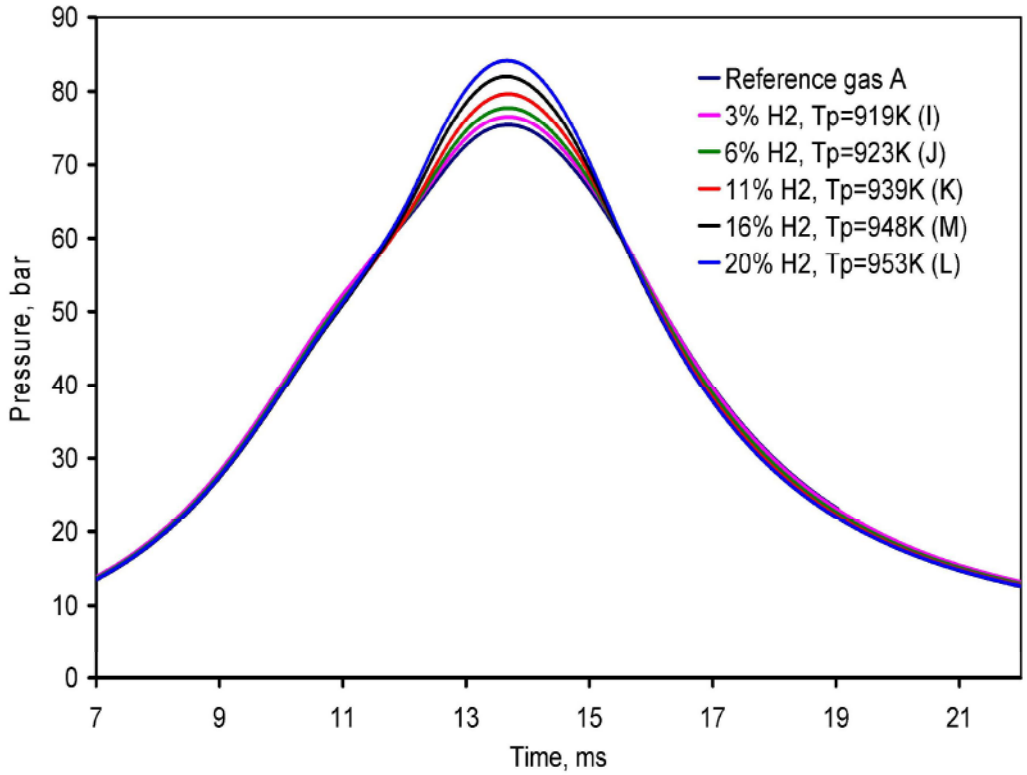

Figure 3: Measured pressure profiles as function of time for G-gas/H_2 gases (table 2). In the legend the derived peak temperatures (T_p) are presented.

The autoignition calculations (figures 4 and 5) show the reduction in knock resistance with increasing fractions higher hydrocarbons and hydrogen in the fuel. The knock resistance measured in the KEMA gas engine via the knock limited spark timing (*KLST*) method is illustrated in the legends of the figures. Taking into account the uncertainty in the measured *KLST* of ±0.5 degree CA we see no difference in the ranking order based on autoignition delay time and *KLST*. To study the relation between autoignition and KLST in more detail the autoignition delay times are derived from figures 4 and 5 by taking 12 ms as an arbitrary zero of time and plotted as function of the KLST in figure 6. From the excellent observed correlation between the KLST and the calculated autoignition delay time (figure 6) we conclude that the used methodology accurately predicts the knock propensity in the used high speed gas engine for all gases tested in this study.

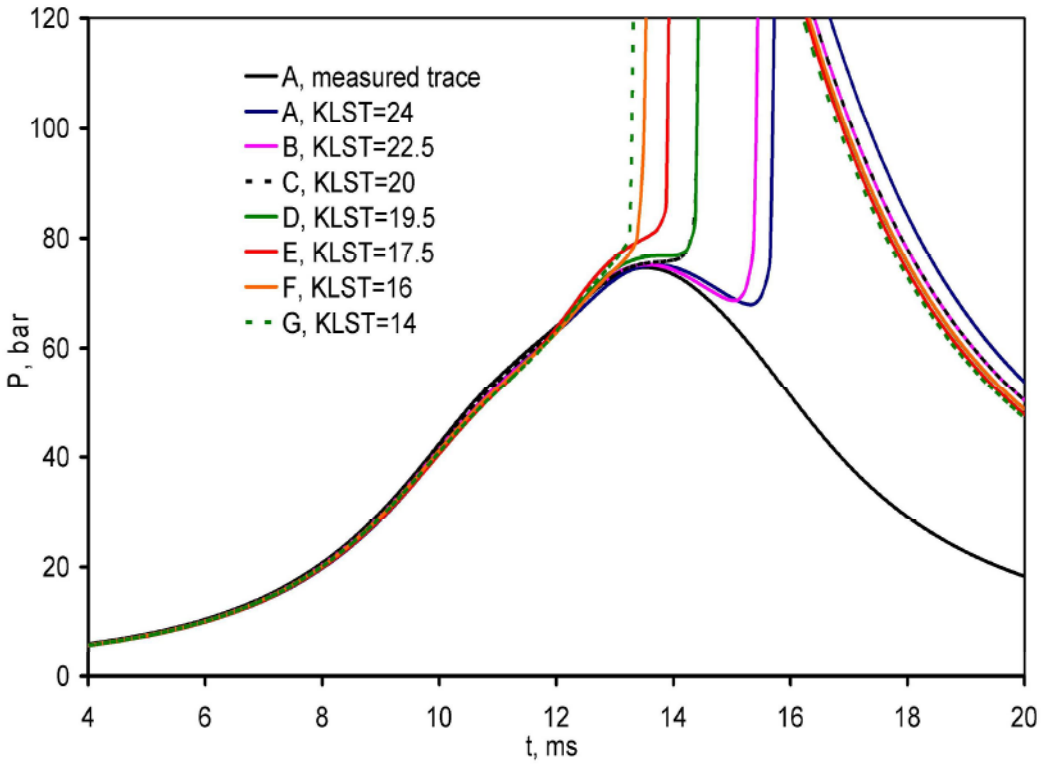

Figure 4. *Ignition of the natural gases (table 1) subjected to the complete measured pressure and temperature history, at (fictive) initial temperature T_0+47K.*

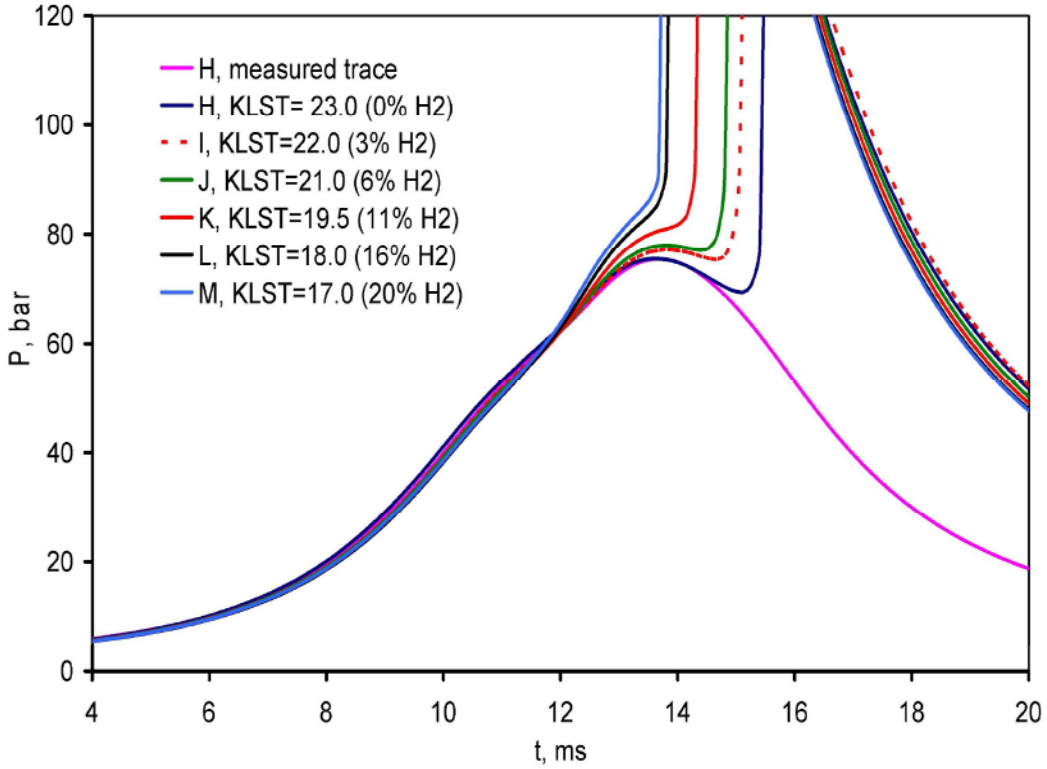

Figure 5. *Ignition of H_2/natural gas mixtures (table 2) subjected to the complete measured pressure and temperature history, at (fictive) initial temperature T_0+47K*

As discussed above, a widely accepted method to rank gases for knock resistance is the Methane Number. For this reason, the relation between the Methane Number calculated via the AVL methodology [2] and the calculated ignition delay time have been investigated and presented in figure 7. As can be seen, an excellent correlation between the methane number and the measured KLST is observed for the Dutch natural gases mixed with different fractions of ethane and propane (table 1) while only a moderate correlation for the Dutch natural gas/H_2 mixtures is found. The relation between the fraction of hydrogen in Dutch natural gas and the Methane Number [2] is also presented in figure 8. From this figure it is clearly seen that the knock resistance calculated with the AVL methane numbers increases with the addition of small fractions of hydrogen to Dutch natural gas (<3% H_2) and subsequently for higher concentration hydrogen in the fuel (>3% H_2) the knock resistance decreases. In contrast, the KLST shown in the same figure decreases nearly linearly with increasing fractions hydrogen in the reference fuel over the entire measured domain, as also observed in [20].

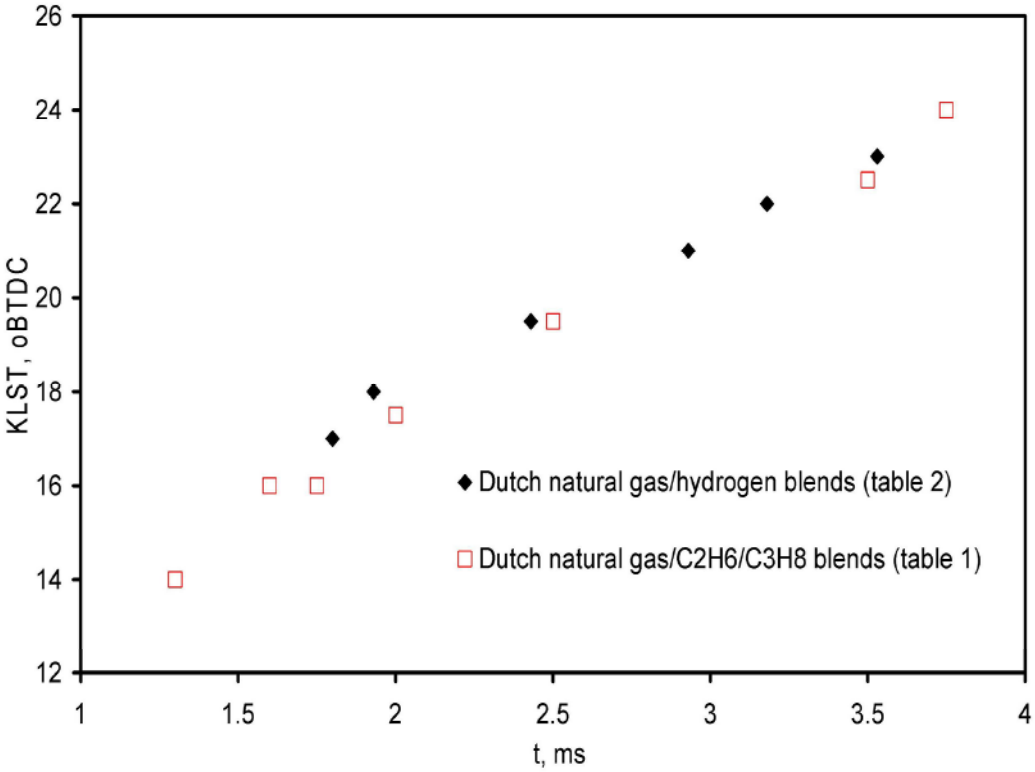

Figure 6: Calculated autoignition delay time based on the complete measured P-T history versus knock limited spark timing (KLST).

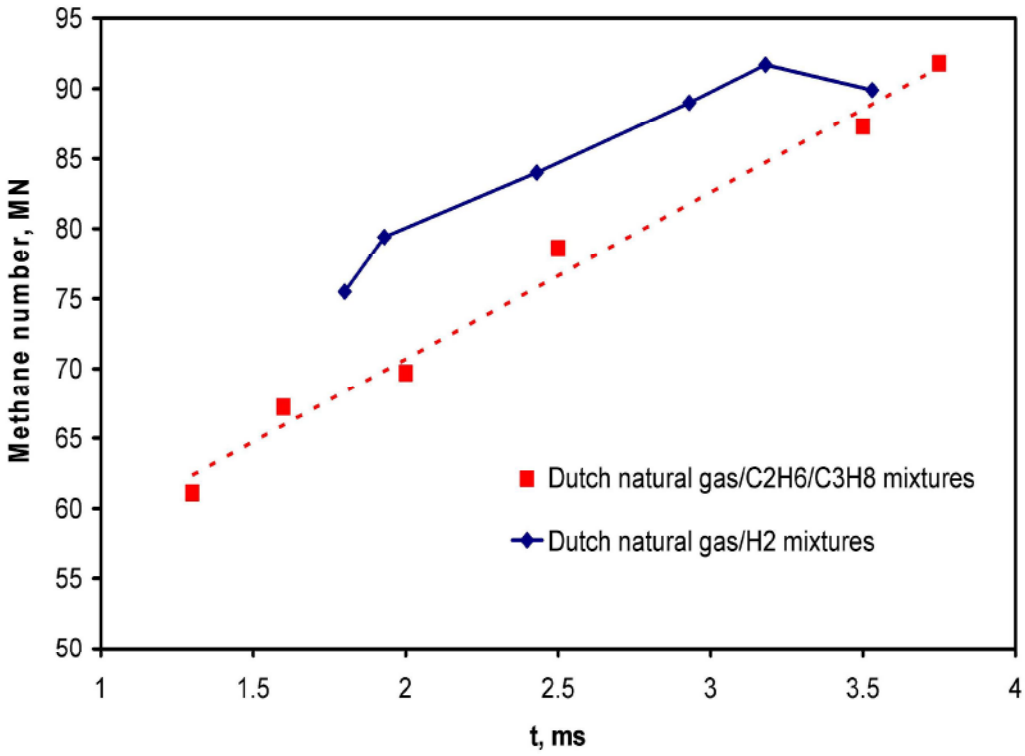

Figure 7: Computed autoignition delay times versus calculated methane number [2] for natural gases (table 1) and natural gas/hydrogen fuel mixtures (table 2).

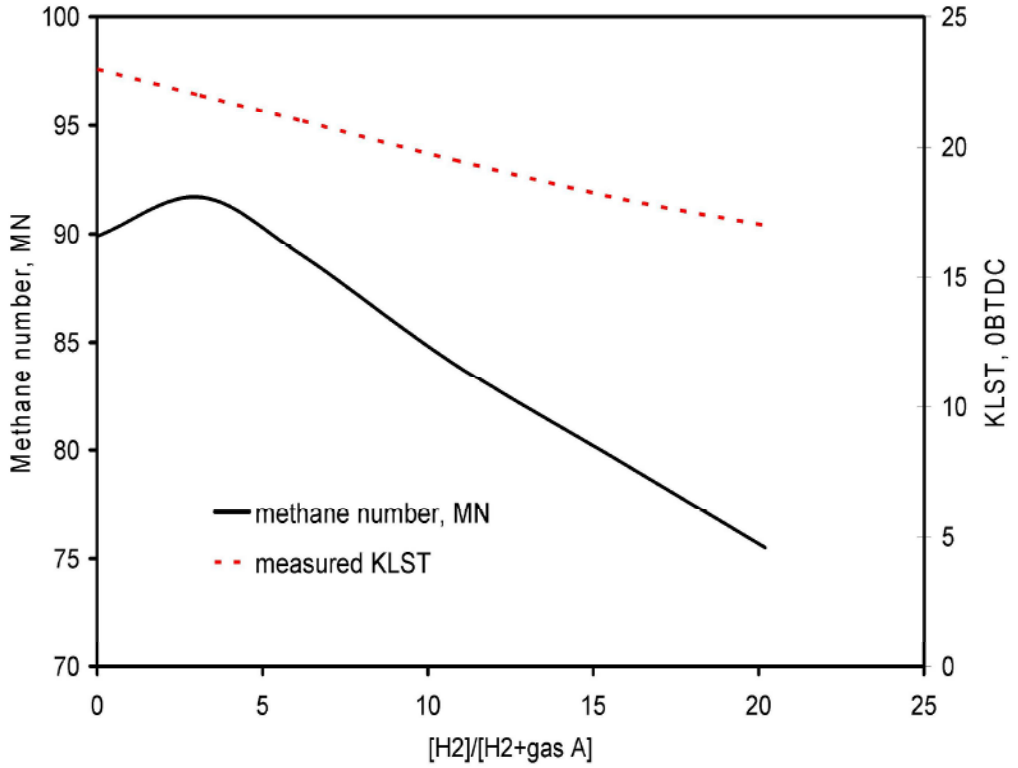

Figure 8: Methane number (AVL) and measured KLST versus hydrogen percentage in reference gas A.

As shown above we are able to predict accurately the knock propensity of gases based on the effective volume derived from the measured pressure profiles at non-knocking condition. In order to calculate the knock propensity based solely on the chemical and physical properties of the gas mixtures it is necessary to predict the changes in the pressure and temperature history (figure 3) upon varying the gas composition. Here, we modeled the pressure and temperature history during the cycle at non-knocking conditions by using an empirically based approach, which we deem adequate for this purpose.

Since we know that the end gas is compressed by both the motion of the piston and the thermal compression of the advancing flame front the changes in the effective peak compression with varying composition at constant engine conditions (λ, *CR*, spark timing, power output etc.) is the result of the changes in the combustion phasing only. To avoid detailed modelling of the combustion phasing, we make use of the observation that the combustion phasing is correlated with the laminar burning velocity [16]. Towards this end, the laminar burning velocity (S_L) of the gases studied (table 1 and 2) are calculated with the PREMIX code [18] from the CHEMKIN suite [17], using a recently developed mechanism [19] and thermodynamic data base [19]. As input into the simulations, the local measured pressures and temperatures conditions at the moment of spark timing (14° CA before TDC) are used. Both the maximum effective compression ratios ($CR_{eff.}$), calculated with equation (1) and (2) by using the measured initial temperature and pressure history, and the computed laminar burning velocities (S_L) of the studied gases are compared relative to those of the reference gas A (Dutch natural gas) and plotted in figure 9. The figure clearly shows a linear correlation between the changes in the maximum measured effective compression ratio ($CR_{eff}/CR_{eff,\ ref}$) and the changes in the laminar burning ($S_L/S_{L,\ ref}$) velocity for both the Dutch natugas/H_2 mixtures and the Dutch natural gas/C_2H_6/C_3/H_8 mixtures. However, the slope of the Dutch natural gas/H_2 mixture is much steeper than that of the Dutch natural gas/C_2H_6/C_3H_8 mixtures. A possible explanation for this observed difference is that for hydrogen containing mixtures the combustion duration of the first ten percent of the mixture (often also referred to as the "ignition delay") is substantially faster than that of the pure natural gas mixtures. Therefore, the initial growth and propagation of the flame front is faster, which would mean that a larger amount of the end gas compression caused by the advancing flame front occurs before the piston reaches top dead centre (*TDC*). This would increase the amount of thermal compression that the end gas of the hydrogen containing mixtures experiences in comparison to pure natural gas mixtures. Another possible explanation is that the relation between the turbulent and laminar burning velocity for hydrogen containing natural gases scales with another scaling factor than the pure natural gases [21]. The understanding in the details of the combustion behaviour of these gases is currently under investigation.

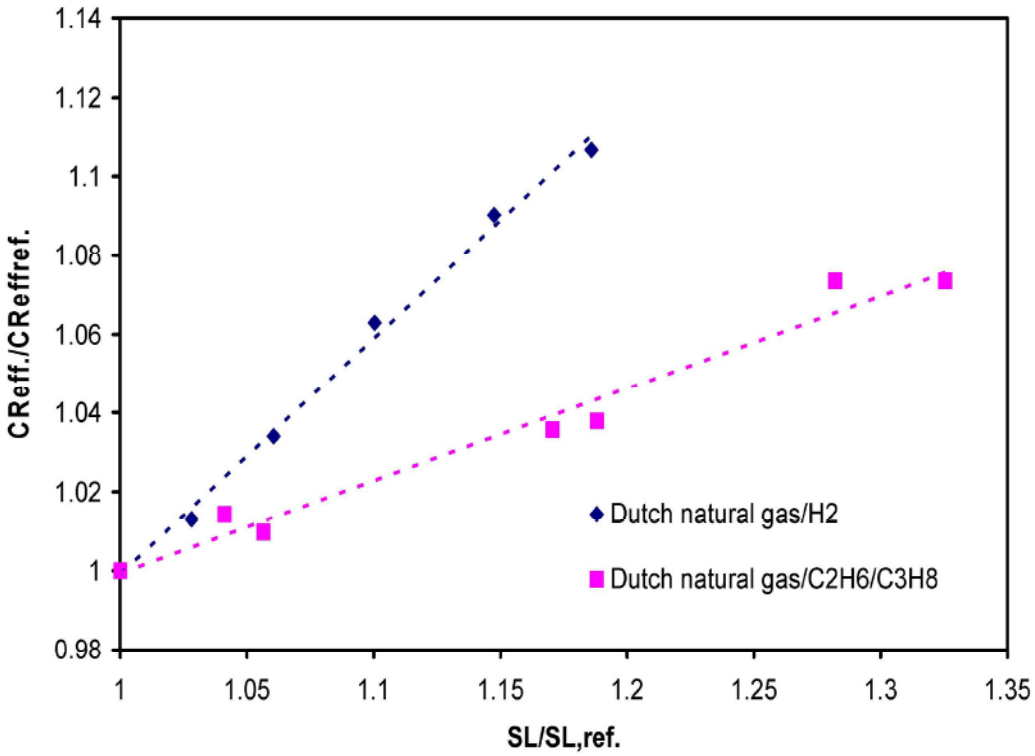

Figure 9: Ratio of the laminar burning speeds relative to gas A (S_L/S_L, ref gas A) as function of the ratio of the effective compression ratio relative to gas A (CR_{eff}/CR_{eff}, ref gas A).

By using the correlations found in figure 9, the known effective compression ratio of reference gas A, the known laminar burning velocity of reference gas A and equations (1) and (2), we now have the means to calculate the peak pressure *(P_{peak})* based on solely the calculated laminar burning velocity of the gas. To model the entire pressure history we make use of a Gaussian expression from which the fit parameters in the expression are derived from both reference gas A (table 1) and the calculated peak pressure *(P_{peak})* of the gas under investigation. As an illustration, the modelled pressure profiles for mixture H (natural gas) and mixture M (20% H_2) are presented in figure 10 and compared with the measured profiles. For the entire set of measured gases, excellent agreement is found between the measured and modelled pressure profiles, as also shown in figure 10. By using the specific volume derived from the modelled pressure traces as input into the simulations we now have the means to predict the knock propensity successfully based on solely the physical and chemical properties of the fuel.

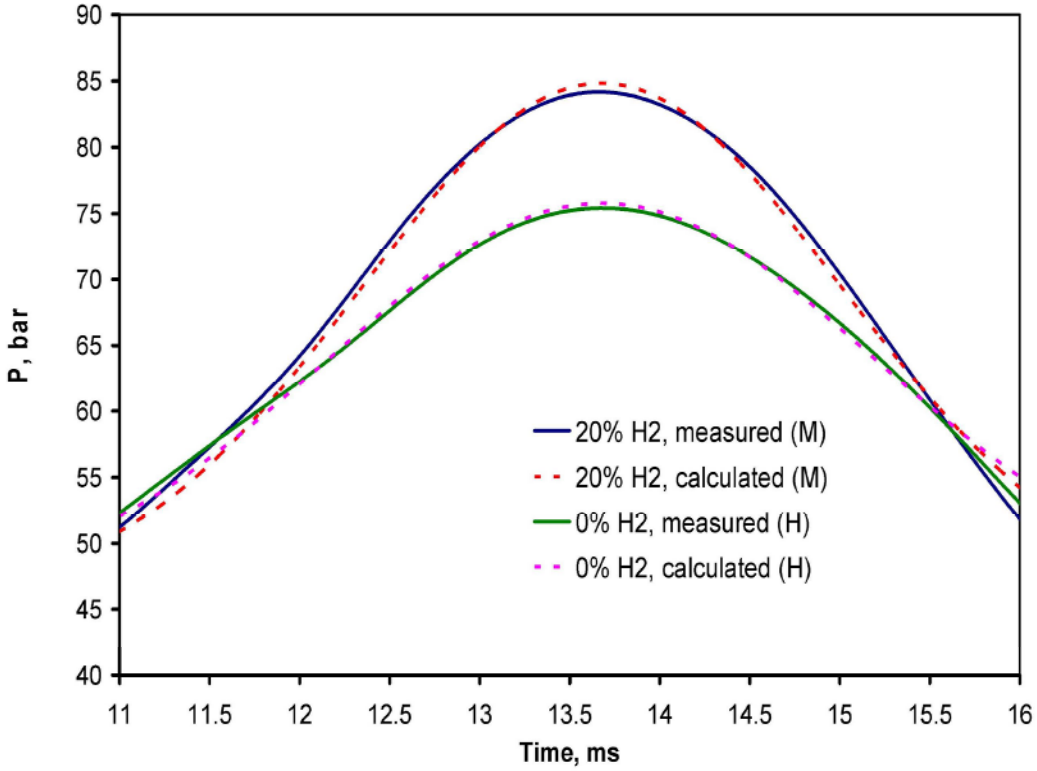

Figure 10: Measured and simulated pressure profiles for gas mixtures H and M.

5 FUTURE WORK

We are currently expanding the analyses described above to a wider range of fuel compositions. The challenge is to predict the combustion phasing as well for combinations of rich natural gases (C1-C5) in combination with hydrogen and CO. Because the timing and pressure/temperature regime is different in large machines (often with pre-chamber combustion), we are planning to validate the method on such an engine.

Acknowledgement

This research has been financed by a grant from the Energy Delta Gas Research (EDGaR) program. EDGaR is co-financed by the Northern Netherlands Provinces, the European Fund for Regional Development, the Ministry of Economic Affairs, Agriculture and Innovation and the Province of Groningen. We gratefully acknowledge the financial support from the N.V. Nederlandse Gasunie.

6 REFERENCES

1. Heywood, J.B., (1989). International Combustion Engine fundamentals, McGraw-Hill
2. Leiker, M., Cartelliere, W., Christoph, H., Pfeifer, U., Rankl, M. (1972). Evaluation of Anti-Knock Property of Gaseous Fuels by Means of the Methane Number and Its Practical Application to Gas Engines. ASME paper 72-DGP-4
3. Spadaccini, L.J., Colket, L.J. (1994). Ignition delay characteristics of methane fuels. Prog. Energy Combust. Sci., Vol 20 pp. 431-460
4 Huang J, Bushe WK, Hill PG, Munshi SR. (2006). Experimental and kinetic study of shock initiated ignition in homogeneous methane–hydrogen–air mixtures at engine-relevant conditions. Int J Chem Kinet 38(4):221–33
5. Petersen, E.L., Kalitan, D.M., Simmons, S., Bourque, G., Curran, H.J., Simmie, J.M. (2007). Methane/Propane Oxidation at High Pressures: Experimental and Detailed Chemical Kinetic Modelling, Proc. Combust. Inst., 31 447-454
6. Lamoureux, N., Paillard, C.E., Vaslier, V. (2002). Shock waves, 11 309-322
7. Levinsky, H.B., Gersen, S., Rotink, M.H., van Dijk, G.H.J. (2008). Towards a rational method for ranking gases for knock resistance using ignition delay times. IGRC Paris
8. Gersen, S., Anikin, N.B., Mokhov, A.V., Levinsky, H.B. (2008). Ignition properties of methane/hydrogen mixtures in a rapid compression machine. Int. J. of Hydrogen Energy 33 1957-1964.
9. Lutz, E., R. Kee, J., Miller, J.A. (1987). SENKIN: A FORTRAN program for predicting homogeneous gas phase chemical kinetics with sensitivity analysis. Sandia Report SAND87-8248. Sandia National Laboratories
10. Donato, N., Aul, C., Petersen, E., Zinner, C., Curran, H., Bourque, G. (2010). Ignition and Oxidation of 50/50 Butane Isomer Blends Journal of Engineering for Gas Turbines and Power Vol. 132 / 051502.
11. Healy, D., Donato, N.S., Aul, C.J., Petersen, E.L., Zinner, C.M., Bourque, G., Curran, H.J. (2010). n-Butane Ignition Delay Time Measurements at High Pressure and Detailed Chemical Kinetic Modeling. Combustion and Flame 157(8):1526-1539.
12. Healy, D., Donato, N.S., Aul, C.J., Petersen, E.L., Zinner, C.L., Bourque, G., Curran H.J. (2010). Isobutane Ignition Delay Time Measurements at High Pressure and Detailed Chemical Kinetic Modeling Combustion and Flame 157(8):1540-1551.
13. Healy, D., Kopp, M.M., Polley, N.L., Petersen, E.L., Bourque, G., Curran, H.J. (2010). Methane/n-Butane Ignition Delay Measurements at High Pressure and Detailed Chemical Kinetic Simulations Energy and Fuels 24(3) 1617-1627.
14. Healy, D., Kalitan, D.M., Aul, C.J., Petersen, E.L., Bourque, G., Curran, H.J. (2010). Oxidation of C1-C5 Alkane Quinternary Natural Gas Mixtures at High Pressures. Energy and Fuels 24(3) 1521-1528.
15. Gersen, S., Darmeveil, H., Levinsky, H.B. (2011). Autoignition delay times of CH_4/CO/H_2 fuels mixtures at high pressure in a RCM. Combustion and Flame to be submitted.
16. Tagalian, J., and Heywood, J.B. (1986). Combustion and Flame, 64: 243-246.
17. Kee, R.J., Rupley, F.M., Miller, J.A. (1989) CHEMKIN II: A Fortran Chemical Kinetics Package for the Analysis of Gas-Phase Chemical Kinetics., Sandia National Laboratories
18 Kee, R.J., Grcar, J.F., Smooke, M.D., Miller, J.A. (1985). Fortran program for modelling steady one-dimensional premixed flames. Sandia Report SAND85-8240. Sandia National Laboratories
19 Bourque, G., Healy, D., Curran, H.J., Zinner, C., Kalitan, D., de Vries, J., Aul, C., and Petersen, E.L. (2008). Ignition and Flame Speed Kinetics of Two Natural Gas Blends with High Levels of Heavier Hydrocarbons, Proc. ASME Turbo Expo., 3:1051–1066
20 Attar, A.A., Karim, G.A.(2003). ASME Transaction, Journal of Gas turbines and power, vol. 125 41-47.
21. Daniele, S., Johansohn, P., Boulouchos, K. (2009). Flame front characteristics and Turbulent flame Speed of lean premixed syngas combustion at Gas Turbine Relevant Conditions. GT2009-59477 ASME Turbo Expo, Orlando